Examining the Crystal, Optical, Transport, and Magnetic Properties of Sb/Ag co–doped SnO_2 Compounds

By

Kuldeep Kumar Singha

Guest Faculty, Department of Physics

Bodoland University



16th Regular Conference of the Physics Academy of the North East (PANE 2026)

Date: 20/11/2026

Introduction

- SnO_2, a remarkable oxide, is used in catalysis, photodiodes, voltage sources, and many other multipurpose systems and devices.
- SnO_2 is an n-type semiconductor with a tetragonal rutile structure ($P4_2/mnm$ space group) with a significant optical band gap of 3.6 eV.
- It was proposed that co-doping elements in SnO_2 compounds could enhance their crystallographic property, Raman spectra, and optical property.



Powder form SnO_2

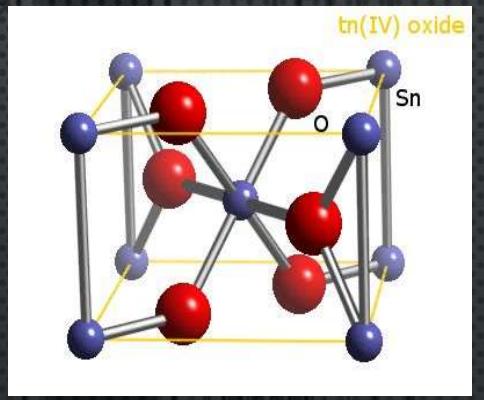

Crystal structure of SnO_2

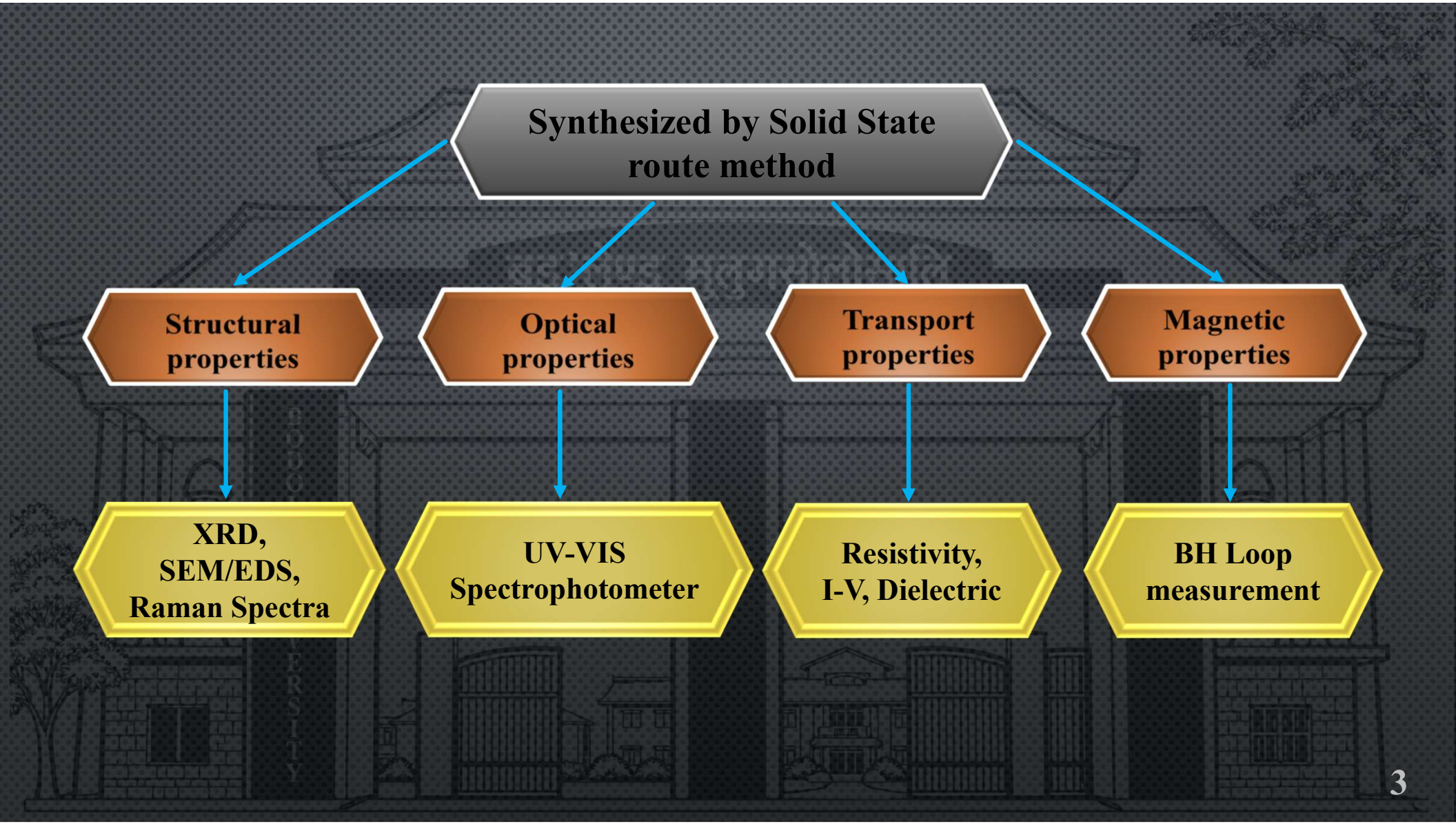
Synthesized by Solid State route method
Structural properties
Optical properties
Transport properties
Magnetic properties
XRD, SEM/EDS, Raman Spectra
UV-VIS Spectrophotometer
Resistivity, I-V, Dielectric
BH Loop measurement

(a) Sample preparation by solid state route method

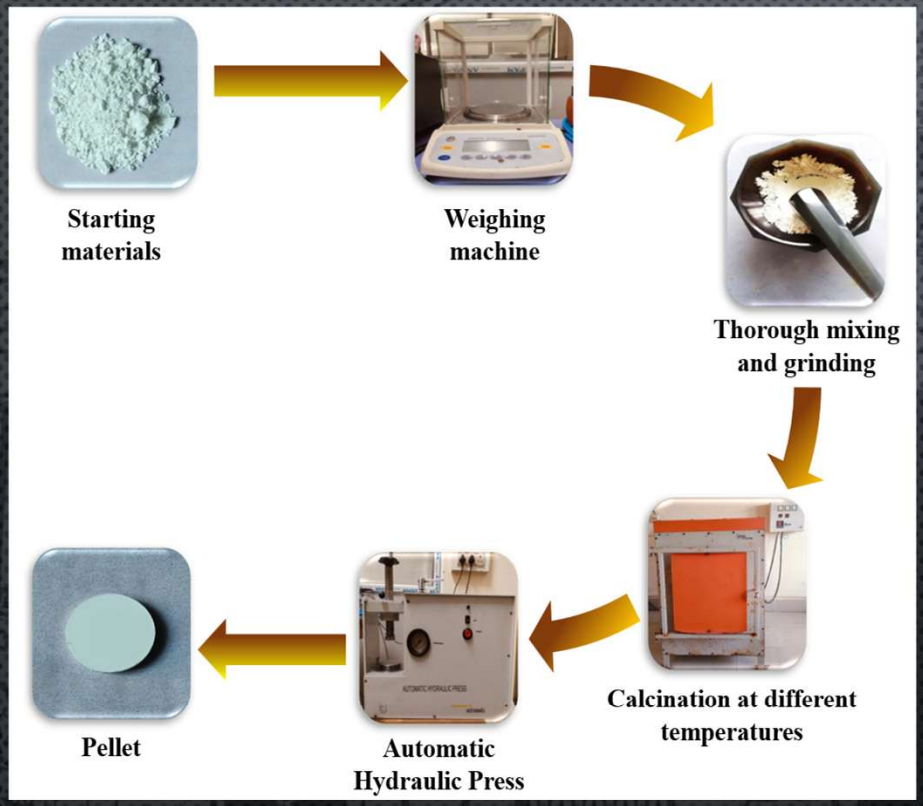

Figure 1: The schematic diagram presents the method of synthesis through solid–state reactions

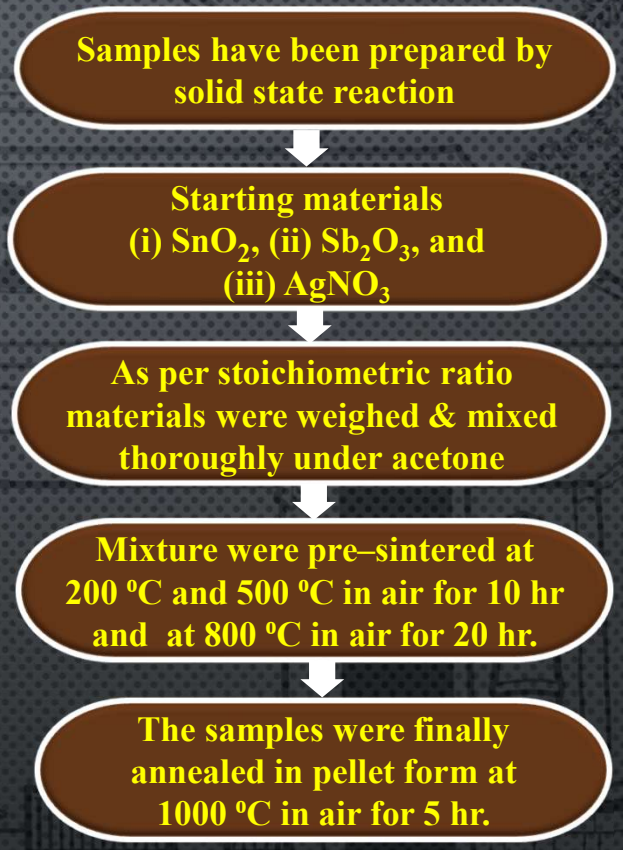

Figure 2: Flowchart summarizing the procedural steps necessary for the solid–state reaction method

(b) Crystal Structure

- The XRD data indicates that the samples were crystallized in a single phase and no secondary phase is present in Ag-Sb:SnO_2 compound.
- The tetragonal rutile-type structure of SnO_2 can be indexed using XRD patterns (space group $P4_2/mnm$, JCPDS card no. 14–1445).

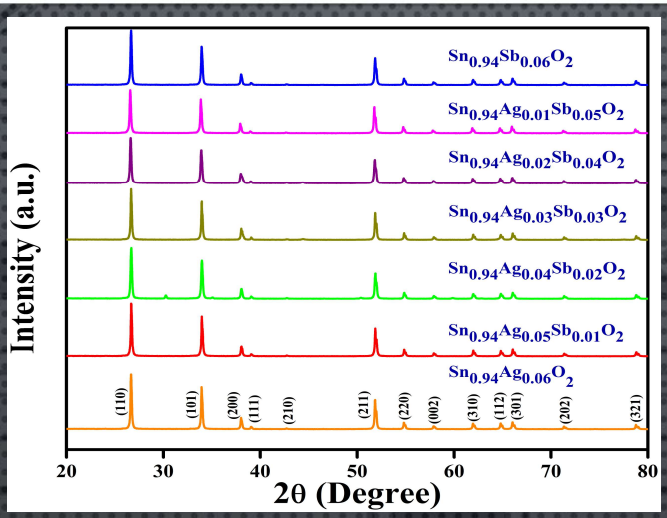

Figure 3: XRD patterns of $Sn_{0.94}Ag_{0.06-y}Sb_yO_2$ ($0 \leq y \leq 0.06$) compounds

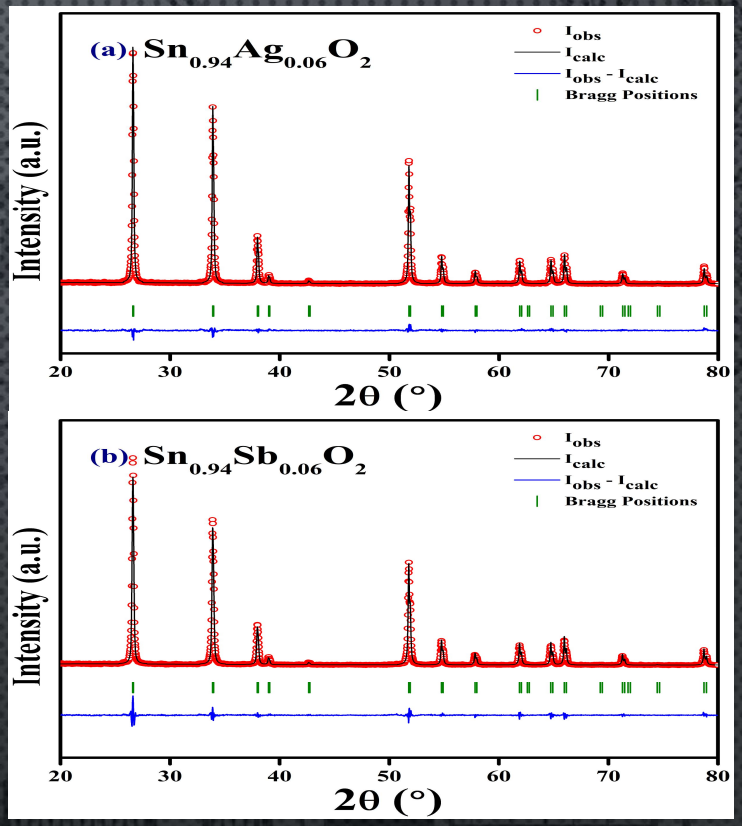

Figure 4: Rietveld refinement XRD patterns of $Sn_{0.94}Ag_{0.06-y}Sb_yO_2$ (y=0, 0.06) compounds

Here, the red circles represent the experimental data;
The solid black solid lines indicate the software calculated intensities;
The lowermost solid blue lines indicate the difference between experimental and software calculated values;
The green vertical short lines indicate the permitted Bragg positions.

(b) Crystal Structure

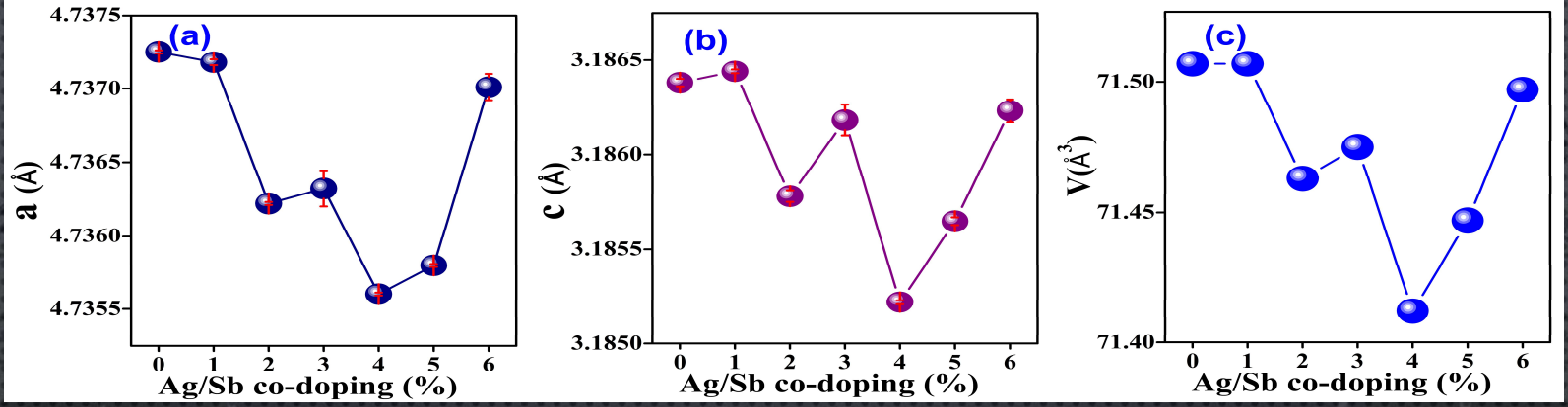

Figure 5: Variation of lattice parameters (a and c) and cell volume (V) along-with error bar of $Sn_{0.94}Ag_{0.06-y}Sb_yO_2$ ($0 \leq y \leq 0.06$) compounds

Substituting Sb and Ag into SnO_2 results in an initial decrease of upto 4% in unit cell volume and lattice parameters due to the smaller ionic radii (Sb^{3+} at 0.76 Å and Ag^{1+} at 1.15 Å) compared to Sn^{4+} (0.69 Å), leading to lattice contraction. Beyond this doping level, a slight increase in lattice parameters suggests that the dopant ions may also occupy interstitial sites, indicating a transition from substitutional to interstitial incorporation at higher doping concentrations.

(c) Micro Structural and EDS Analysis

- SEM analysis revealed nano–sized, circular grains with nano–range particle size.
- The particle sizes have been determined to be 60 nm and 50 nm for $Sn_{0.94}Ag_{0.02}Sb_{0.04}O_2$, and $Sn_{0.94}Sb_{0.06}O_2$ compounds.
- EDS analysis shows a uniform distribution of all elements across the samples.

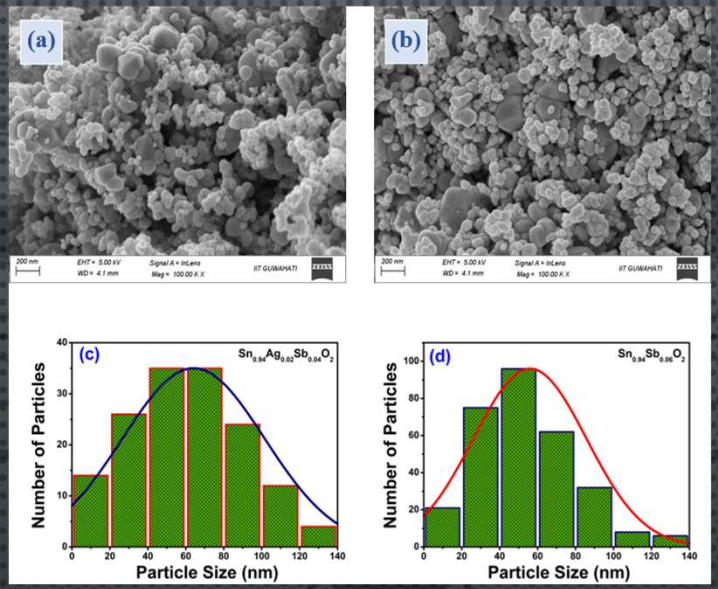

Figure 6: The micro–structural images for $Sn_{0.94}Ag_{0.02}Sb_{0.04}O_2$, and $Sn_{0.94}Sb_{0.06}O_2$ compounds

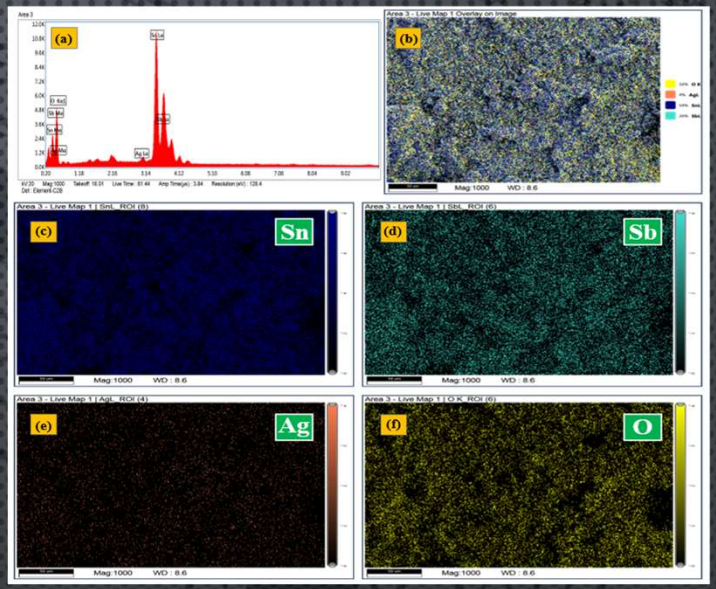

Figure 7: The energy dispersive spectra (EDS) and elemental color mapping of $Sn_{0.94}Ag_{0.02}Sb_{0.04}O_2$ compound displays the individual elements as Sn, Sb, Ag, and O

(d) Raman analysis

- A_{1g} mode at 632 cm^{-1} (symmetric Sn–O stretch), B_{2g} mode at 773 cm^{-1} (asymmetric Sn–O stretch), and E_g mode at 473 cm^{-1} (O–O stretch).
- Additional peaks at 249 and 284 cm^{-1} assigned to E_u (TO) and E_u (LO).
- Peak intensities peaked at 5–6% doping.
- Crystalline structure enhancement likely caused increased peak intensity.
- Raman spectra confirm tetragonal rutile SnO_2 phase and successful Ag–Sb incorporation.

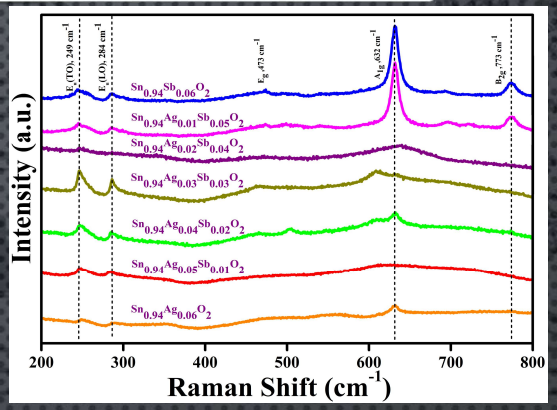

Figure 8: Raman spectra of $Sn_{0.94}Ag_{0.06-y}Sb_yO_2$ ($0 \leq y \leq 0.06$) compounds

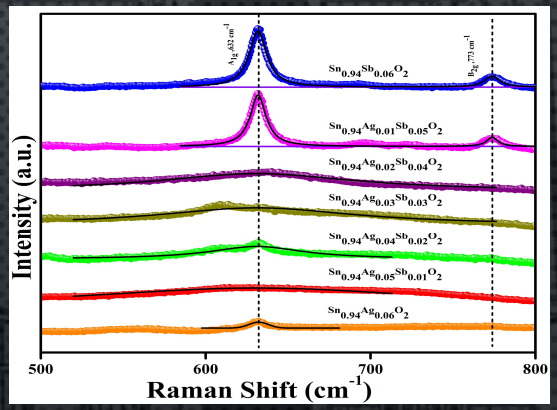

Figure 9: Lorentzian fitting of the $Sn_{0.94}Ag_{0.06-y}Sb_yO_2$ ($0 \leq y \leq 0.06$) Raman spectrum

(e) Optical property

- The spectra display a UV absorption edge at 255 nm for all the samples.
- From transmittance spectra, $Sn_{0.94}Ag_{0.06-y}Sb_yO_2$ ($0 \leq y \leq 0.06$) compounds appear almost transparent in the visible region (350–800 nm).
- The optical band gap decreases with increasing co-doping concentration, which may due to the formation of narrow impurity bands inside the prohibited gap region.

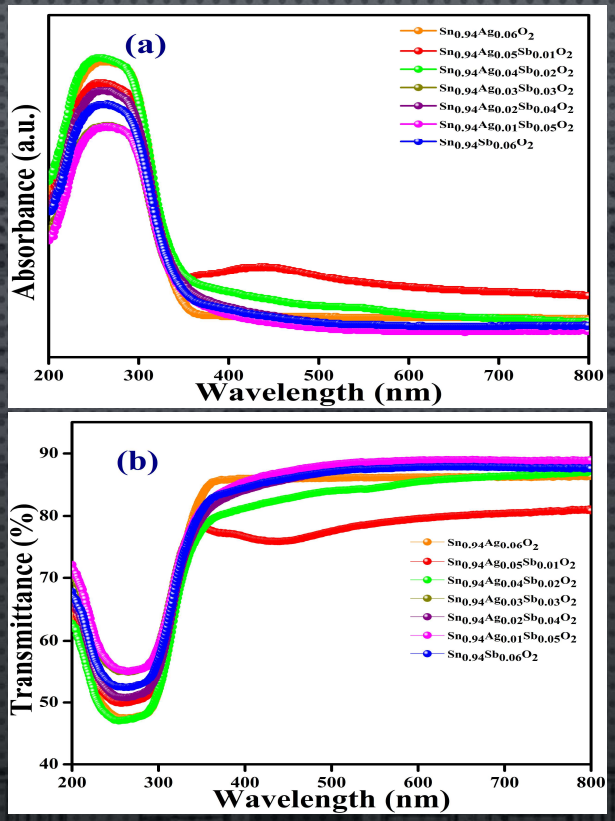

Figure 10: UV-Visible (a) absorbance & (b) transmittance spectra of $Sn_{0.94}Ag_{0.06-y}Sb_yO_2$ ($0 \leq y \leq 0.06$) compounds

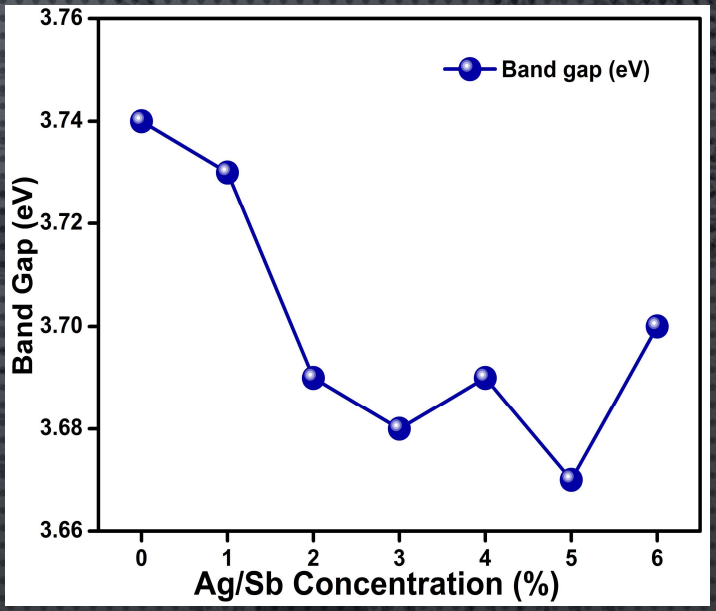

Figure 11: Variation of band-gap for $Sn_{0.94}Ag_{0.06-y}Sb_yO_2$ ($0 \leq y \leq 0.06$) compound

(f) Resistivity measurement

- Resistivity was measured at 30–100 °C under constant current, showing a linear trend in semilogarithmic plots.
- At 300 K, resistivity decreases from 942.83 Ω·cm ($Sn_{0.94}Ag_{0.06}O_2$) to 769.79 Ω·cm ($Sn_{0.94}Ag_{0.05}Sb_{0.01}O_2$), and further from 4.349 Ω·cm to 1.274 Ω·cm as Sb content increases for $y \geq 0.02$.
- This trend demonstrates that doping concentration significantly influences the electrical properties of these materials.

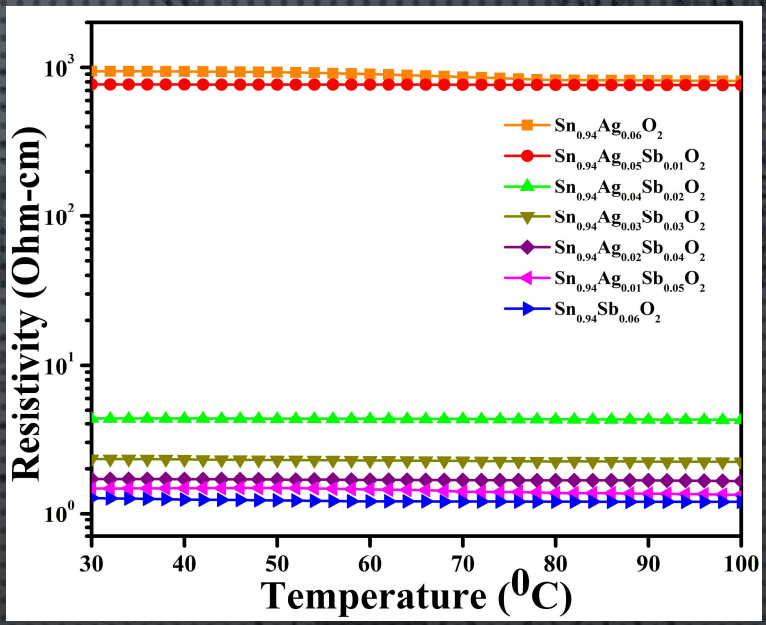

Figure 12: Temperature dependence of electrical resistivity for $Sn_{0.94}Ag_{0.06-y}Sb_yO_2$ ($0 \leq y \leq 0.06$) compounds

(g) I-V Characteristics

- $Sn_{0.94}Ag_{0.06}O_2$ shows ohmic behavior within the voltage range of 0 V to 100 V.
- Introducing Sb into the compound significantly increases leakage current.
- The increase in leakage current is attributed to a slight decrease in band gap energy and enhanced electrical conductivity, reducing dielectric properties of the material.

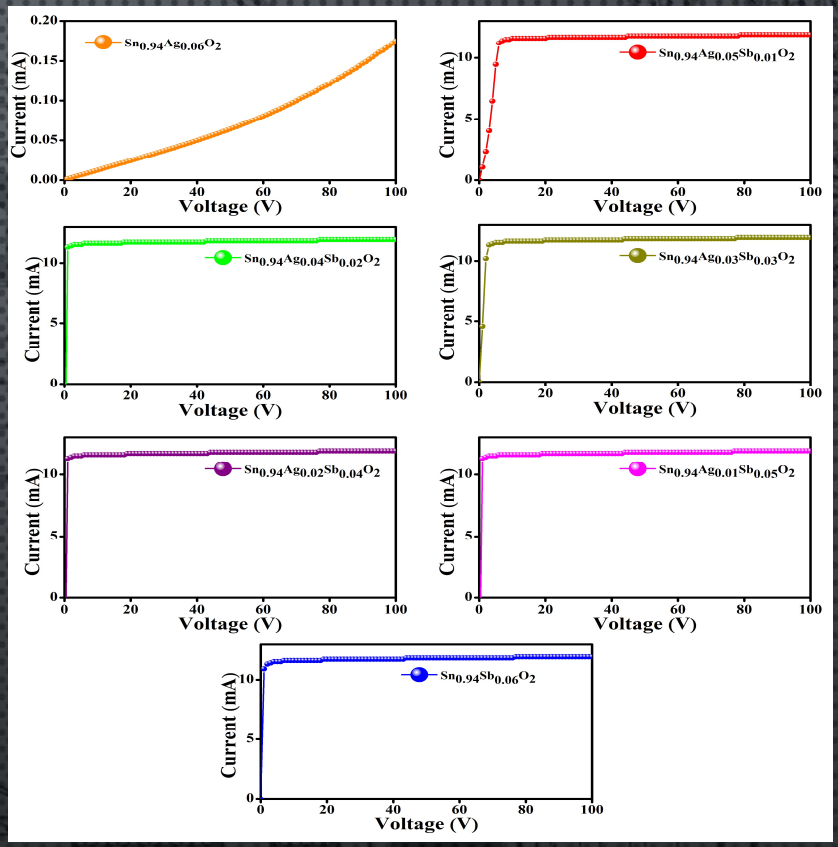

Figure 13: I–V characteristics for $Sn_{0.94}Ag_{0.06-y}Sb_yO_2$ ($0 \le y \le 0.06$) compounds

(h) Dielectric Properties

- Only $Sn_{0.94}Ag_{0.06}O_2$ and $Sn_{0.94}Ag_{0.05}Sb_{0.01}O_2$ show notable frequency-dependent dielectric behavior at 300 K.
- Dielectric constant (ε_r) and Dielectric loss (tan δ) decreases with increasing frequency, flattered at higher frequencies up to 10 kHz.
- At high frequencies, dipoles can't align quickly, reducing polarization, dielectric constant, and loss.

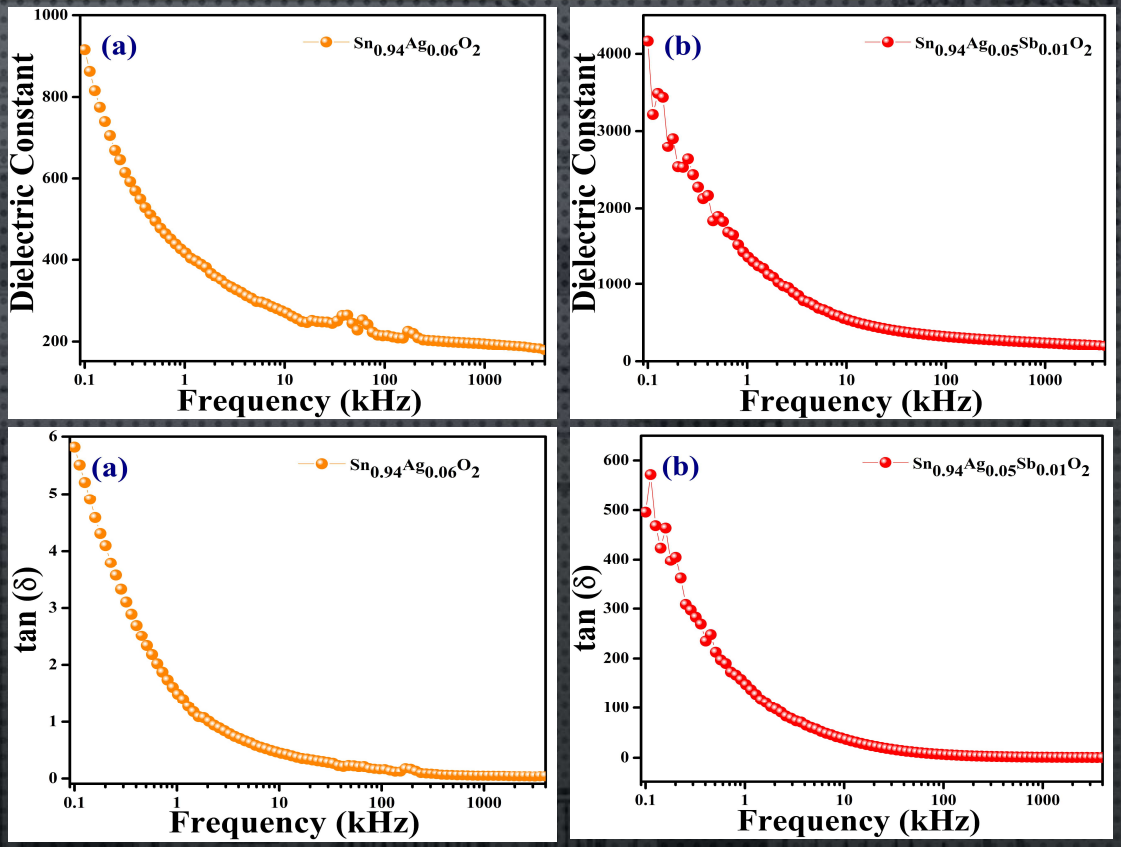

Figure 14: The room temperature frequency variation of dielectric constant and tan δ for (a) $Sn_{0.94}Ag_{0.06}O_2$ and (b) $Sn_{0.94}Ag_{0.05}Sb_{0.01}O_2$ compounds

(h) Dielectric Properties

- $Sn_{0.94}Ag_{0.06}O_2$ has a large semi-circular arc (high resistance), while $Sn_{0.94}Ag_{0.05}Sb_{0.01}O_2$ has a smaller semi-circular arc (low-resistance).

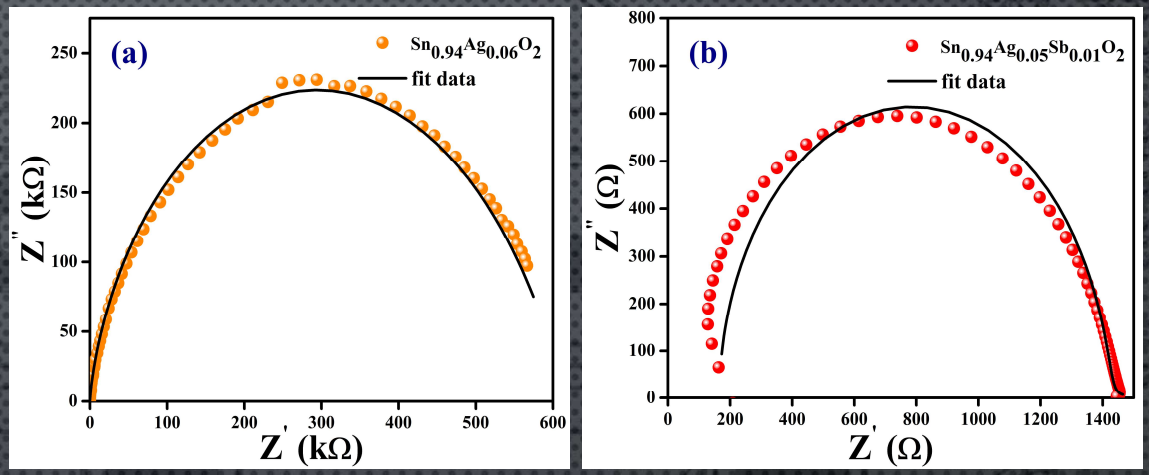

Figure 15: The room temperature frequency variation of Nyquist plot with fitting for (a) $Sn_{0.94}Ag_{0.06}O_2$ and (b) $Sn_{0.94}Ag_{0.05}Sb_{0.01}O_2$ compounds

Sample/ Parameters	R_s (kΩ)	C_{gb} (nF)	R_{gb} (kΩ)
$Sn_{0.94}Ag_{0.06}O_2$	-------	0.07962	618.2
$Sn_{0.94}Ag_{0.05}Sb_{0.01}O_2$	0.1656	0.1682	1.333

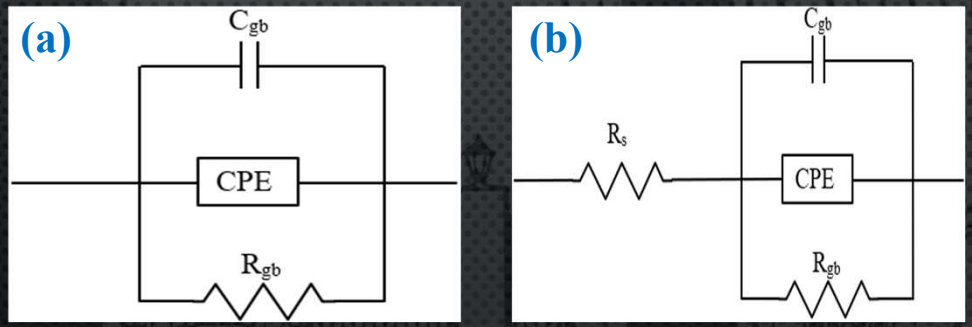

Figure 16: The Equivalent circuit model for Nyquist Plot of $Sn_{0.94}Ag_{0.06-y}Sb_yO_2$ ($0 \leq y \leq 0.01$) compounds

(h) Dielectric Properties

- Incorporating Sb enhances AC conductivity, indicating the importance of charge carrier hopping.
- At low frequencies, AC conductivity remains low due to slower charge carrier hopping rates.
- Higher AC frequencies increase the hopping rate, improving charge mobility and significantly boosting AC conductivity.

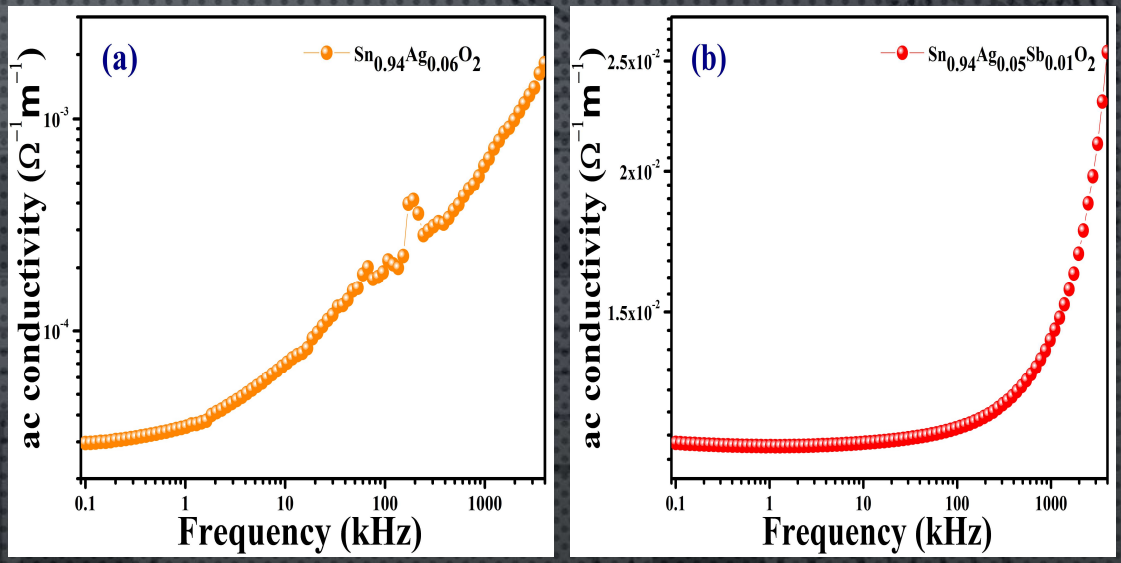

Figure 17: The room temperature frequency variation of ac conductivity for (a) $Sn_{0.94}Ag_{0.06}O_2$ and (b) $Sn_{0.94}Ag_{0.05}Sb_{0.01}O_2$ compounds

(i) B-H Loop measurement

- B–H hysteresis loop for Ag-Sb co-doped SnO_2 compounds, indicating ferromagnetic behavior.
- Coercivity values range from 554.5 to 581 Oe across different doping levels.
- The coercivity behavior reflects a complex, nonlinear response to doping concentration, balancing benefits and potential degradation of magnetic properties.

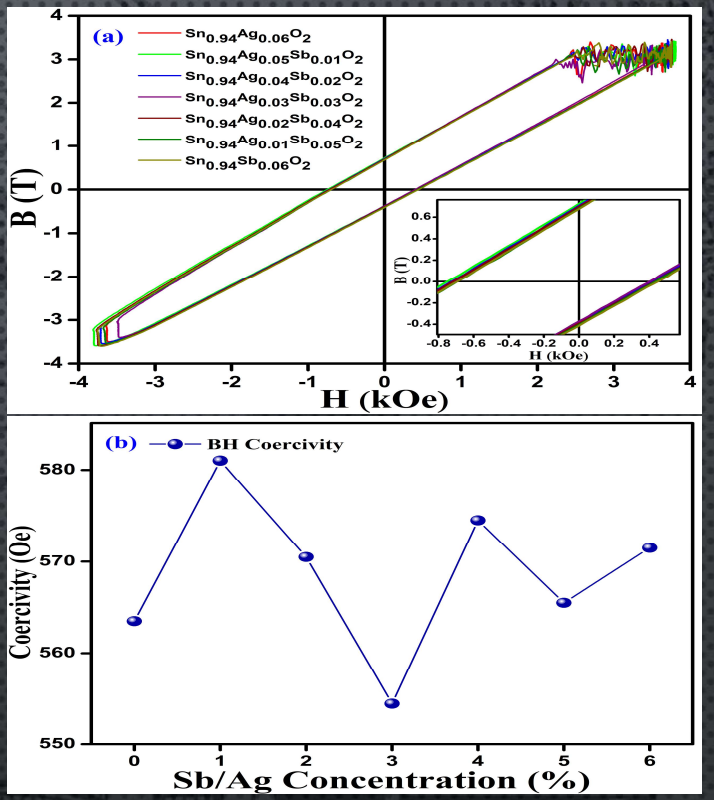

Figure 18: (a) BH loop of $Sn_{0.94}Ag_{0.06-y}Sb_yO_2$ ($0 \le y \le 0.06$) compounds
(b) Variation of coercive field for $Sn_{0.94}Ag_{0.06-y}Sb_yO_2$ ($0 \le y \le 0.06$) compounds

Summary of results obtain in Ag/Sb co-doped SnO_2

- XRD analysis reveals that the samples were crystallized in a single rutile phase with tetragonal structure.
- The SEM analysis reveals that the sample has a uniform morphology with an average particle size of 55–65 nm.
- Raman spectrum also indicates that the tetragonal rutile crystal structure is present in the material.
- The optical band gap was found to decrease with increasing Sb doping concentration.
- Increasing co-doping concentration reduces resistivity from 942.83 to 1.274 Ω·cm, enhancing electrical conductivity from monovalent (Ag^{1+}) to trivalent (Sb^{3+}) transition.
- This increased conductivity correlates with higher leakage currents and a reduction in dielectric properties.
- $Sn_{0.94}Ag_{0.06-y}Sb_yO_2$ (with $0 \leq y \leq 0.06$) compound exhibits ferromagnetism with coercivity ranging from 554.5 to 581 Oe.

“TFM” Research Group @CITK










THANKS!!!